JOURNAL OF MATERIALS SCIENCE 21 (1986) 917–922

Effects of trace impurities on the adherence of oxide to ultra low carbon steel

MICHIHIKO INABA, KOICHI TESHIMA, YOSHINORI HONMA, TSUTOMU YAMASHITA, ISAO SUZUKI, MASAHARU KANTO
Materials Application Department, Toshiba Research and Development Centre, Toshiba Corporation, 1 Komukai Toshiba-cho, Saiwai-ku, Kawasaki-shi, Kanagawa-ken, Japan

The effects of trace impurities on the adherence of oxides to ultra low carbon steels were investigated. Three steels, of differing chromium, aluminium, silicon, nitrogen and oxygen content, were oxidized at 850 K in 10% CO_2–90% N_2 gas and then oxidized at 770 K in 10% CO_2–10% O_2–80% N_2 gas. Surface analysers, i.e. a Mössbauer spectrometer, Auger electron spectrometer and/or ion micro analyser, were utilized in the present study because of the very thin layer of oxides formed (1.0 to 2.0 μm). The following results were obtained. The oxide on the Al-containing steel spalled at the outer–inner oxide interface, where aluminium was enriched and many cavities appeared. The inner oxide layer, oxidized by the transport of CO_2 or O_2 gases along the outer layer grain boundaries or micropores, became thick. This generated a stress at the outer–inner layer interface with the resultant formation of cavities. On the other hand, the oxide on the Cr-containing steel showed good adherence to the metal. The inner layer, enriched with chromium, did not become thick and had no cavities at the interface. The addition of chromium to the Al-containing steel resulted in good oxide adherence because chromium acted as a barrier to the aluminium enrichment.

1. Introduction

Many investigations concerning the oxidation of carbon steels have been performed for a variety of environments (CO_2, O_2, H_2O, air etc.) and temperatures [1–7]. According to these papers, voids or cavities can exist in the oxide layer or at the oxide–metal interface, so that oxides can lose adherence and occasionally spall [1–6]. Investigators have tried to relate these phenomena to such variables as surface roughness, amount of rolling, impurities, specimen geometry, in-diffusion of gas, injection of vacancies into the metal or out-diffusion of iron atoms, etc. [1–9]. However, most of this work has been done on steels containing a few hundred p.p.m. carbon, mainly to study the effect of carbon content on the void formation, or to study the thick oxide layers formed with the scanning electron microprobe (SEM) or the optical microscope (OM).

In recent years, because of improvements in smelting techniques, ultra low carbon steels containing very low impurity levels have become readily available (especially in electronic components). However, these impurities in steels were remarkably enriched at the surface or grain boundaries on annealing in a variety of gaseous environments (vacuum, H_2, N_2, etc.), so that chemical properties (on oxidation, plating, coating with paint) or mechanical properties were affected by these enrichments [10]. So far as oxidation is concerned, it is generally considered that the enrichment of chromium, aluminium and silicon at the steel surface can decrease the oxidation rate constant because these elements form thin protective oxides which inhibit the transport of oxidizing agents. On the other hand, it has also been reported that additions of some impurities (for example silicon) increase the oxidation rate constant (especially in wet gas) [11, 12]. These differential results can be explained by the difference in the amount or kind of enriched impurities at the surface or the grain boundaries.

To investigate the enrichment of impurities, new analytical equipment has been developed. These are useful tools to use in clarifying the above problem. This paper describes the results of a study, which makes use of some of this new analytical equipment, of the effects of trace levels of impurities, primarily aluminium and chromium, on the adherence of the thin oxide layer formed on these low carbon steels; it also clarifies the relation between the impurity enrichment and the adherence of the oxides.

2. Experimental conditions

Cold rolled ultra low carbon steels of three compositions, 0.2 mm thick, were utilized in this study. The three steels varied in regard to the amount of chromium, aluminium, silicon, nitrogen and oxygen present, as shown in Table I. In this work, each steel was provisionally designed as "Cr-steel", "Cr–Al-steel" and "Al-steel", respectively, according to its content. Fig. 1 shows the steps in the preparation of the samples. The three steels were degreased by trichloroethylene to preclude surface contamination, washed in an ethylalcohol bath, followed by immersion in a purified water ultrasonic bath. The surface cleanliness was confirmed with the scanning Auger

0022–2461/86 $03.00 + .12

TABLE I Chemical composition of steels (p.p.m.)

Element	Steel		
	Cr-steel	Al-steel	Cr–Al-steel
C	55	39	36
Si	< 10	130	40
Mn	2350	2660	2870
P	161	153	157
S	130	191	228
Cr	489	74	182
Al	< 1	397	479
Ni	148	146	164
Cu	40	40	40
V	< 5	< 5	< 5
Mg	< 1	< 1	< 1
Na	< 1	< 1	< 1
K	< 1	< 1	< 1
Ca	< 2	< 2	< 2
N	10	46	47
O	338	64	57
Fe	Balance	Balance	Balance

electron microprobe (SAM, Perkin Elmer Co. SAM-590A) and/or ion micro analyser (IMA, Hitachi Ltd. IMA-2). These steels were annealed at 1000 K in an H_2 atmosphere (dew point, 290 K) for 3600 sec to relieve the cold rolling stress and to enrich impurities at the surfaces. These were then oxidized at 850 K in a mixture of 10% CO_2–90% N_2 gas (dew point, 313 K) for 300 sec and at 770 K in a mixture of 10% CO_2–10% O_2–80% N_2 gas (dew point, 313 K) for 120 sec.

These oxidized samples were then evaluated as follows:

1. The oxidized samples were broken in liquid N_2 and the fractured surfaces and the related adherence of the oxides were studied with SEM. This is a simple and suitable method to evaluate the oxide adherence and to consider the reaction of oxides and metals by observing their interfaces.

2. The structure and crystal anisotropy of the oxides were examined with a X-ray diffractometer (XRD) and/or conversion electron Mössbauer spectrometer (CEMS).

3. The diffusion of impurities in the steels to the oxide or the oxide–metal interface zone was analysed with SAM and/or IMA.

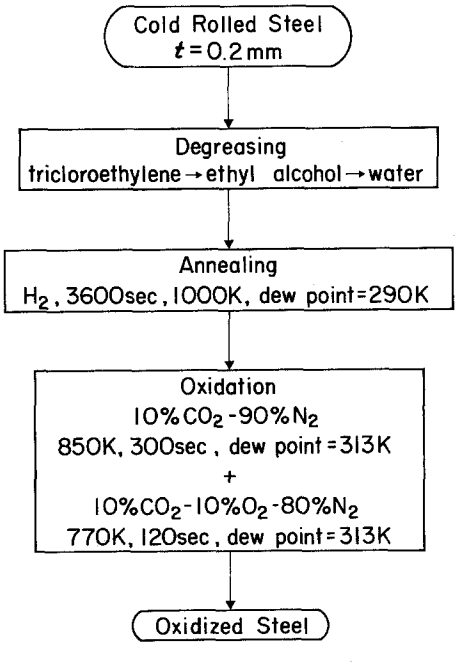

Figure 1 Sample production process.

3. Results

3.1. Properties of oxidized steel

Fig. 2 shows SEM fractographs of the three oxidized steels. The adherence of the oxide is best for the Cr-steel. With the Al-steel, the oxide obviously consists of a double layer as indicated by the inner oxide layer grown remarkably at the interface between the spalled outer oxide layer and the metal. This outer layer is considered to be brittle due to the number of areas where it has spalled. The oxide on the Cr–Al-steel exhibits superior adherence to that for the Al-steel but not as good as that for the Cr-steel.

The thickness of the oxide on the three steels is in the range of 1.0 to 2.0 μm as determined by SEM from sample cross-sections. The Al-steel had the thickest oxide layer, due to the presence of the relatively thick inner oxide layer. Conversion electron Mössbauer spectra (CEM spectra) and XRD data suggested that the oxide consisted of a double layer α-Fe_2O_3 and Fe_3O_4 structure. FeO did not form under these oxidizing conditions. When the oxidized steel was measured by CEMS at the upper most surface, peaks identified as Fe_3O_4 appeared in the spectra. Because of the escape depth of the K-shell conversion electron is under 0.1 μm [13], the above mentioned CEMS results suggested that the thickness of the α-Fe_2O_3 layer was less than 0.1 μm and that most of the oxide consisted of Fe_3O_4. Furthermore, the colour of the sample surface was nearly black, the colour of Fe_3O_4 [14]. With regard to the orientation of the crystal of Fe_3O_4 or the metal, no remarkable differences in anisotropy were observed among the three samples.

Detailed examination of the oxide–metal interface of the Al-steel indicates better adherence in some areas (Fig. 3a) than in others (Fig. 3b). No cavities were observed at the oxide–metal interface (actually, it is the outer–inner oxide interface, as indicated previously) where the oxide adherence was good, while many cavities were observed in areas where adherence was poor. Within the oxide, many voids (indicated by the arrow in Fig. 3) were observed. No voids or cavities were observed on the Cr-steel sample studied in a similar fashion. Furthermore, it was noted that the number of voids and cavities increased with an increase in the ratio of aluminium content to chromium content in these steels. These results suggest that the adherence of the oxide to these steels may depend on the ratio of aluminium to chromium content. Upon analysing the elements at the oxide–metal interface with SAM, aluminium, carbon, oxygen and iron were detected. Fig. 4 shows the depth profile of the detected aluminium KLL–Auger electron peak intensity, divided by the iron LMM–Auger peak, as a function of the sputter-etching time by argon ion gun. It is clear that aluminium is enriched in the cavity area of the oxide–metal interface of the type shown in Fig. 3b, but the chemical state of aluminium was not

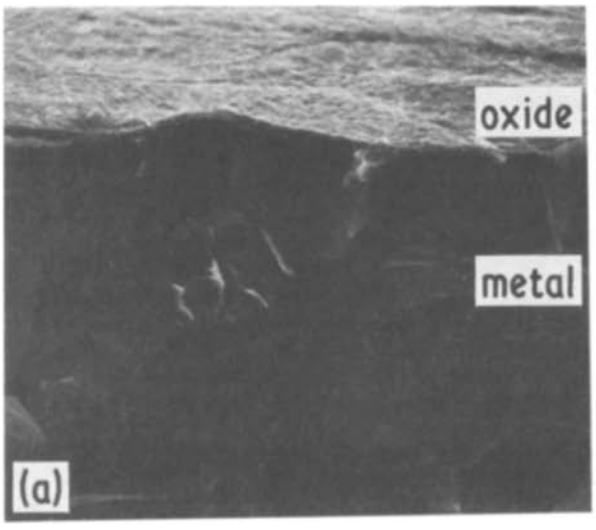

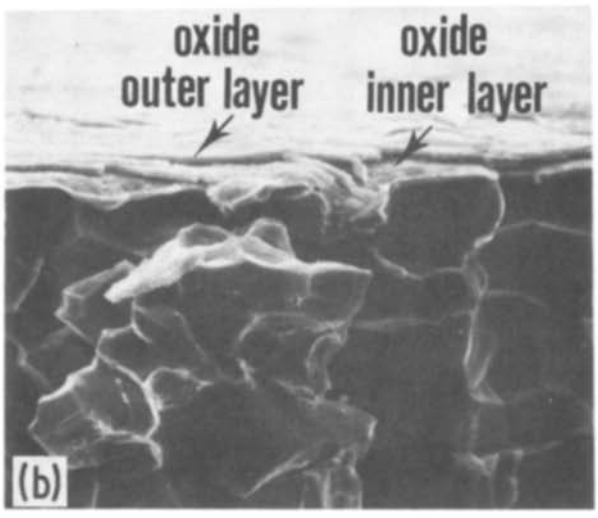

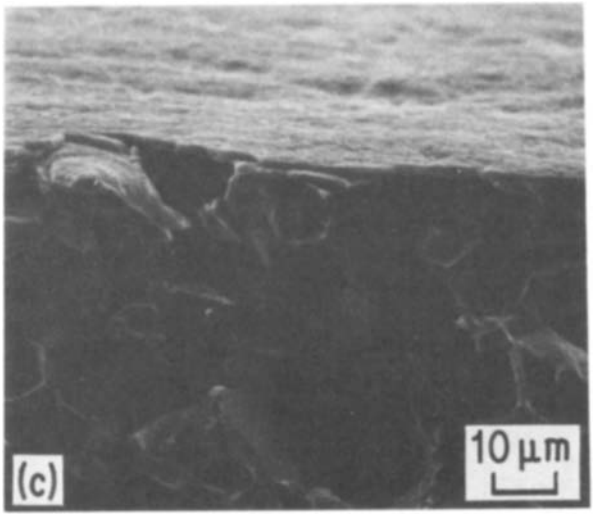

Figure 2 SEM fractographs of oxidized steels. (a) Cr-steel, (b) Al-steel and (c) Cr–Al-steel.

clearly identified. An O KLL–Auger peak in the cavity area was also detected. This suggests that the Fe_3O_4 (oxide on steel) consists of double layers and that the spallation point is this interface between the outer and the inner oxide layers as indicated previously in Fig. 2. With a good adherent oxide layer, as shown in Fig. 3a, aluminium was not enriched at this interface.

3.2. Influence of impurities on the adherence of oxides

Aluminium was enriched in the inner oxide layer in some areas on the Al-steel sample, while other impurities seemed to be uniformly distributed. It is not clear what factors caused the aluminium enrichment. IMA was utilized for obtaining the depth profiles of various elements.

Before obtaining the profiles of the oxidized steels, the surface enrichment phenomena for the annealed steels were analysed with IMA. Table II shows the ratios of the ion peak intensity for several enriched elements to that for $^{57}Fe^+$ at the surfaces of annealed steels (the peak intensity $^{57}Fe^+$ is determined at 1000 in this table). The concentration of aluminium at the Al-steel surface shows a value two hundred times as great as that at the Cr-steel surface. On the other hand, the concentration of chromium at the Cr-steel surface shows a value one hundred times as much as that at the Al-steel surface. It was not believed that silicon and other elements which enriched similarly to each other in each steel, were primarily responsible for the spallation phenomenon. It is therefore significant

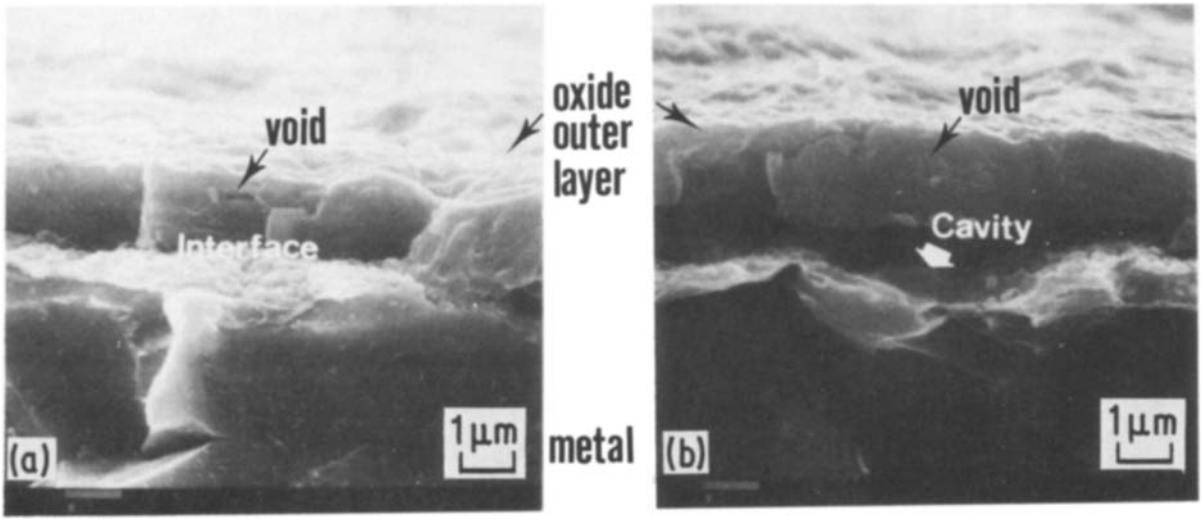

Figure 3 SEM fractographs of oxidized Al-steel at the interface, (a) without cavity, and (b) with cavity.

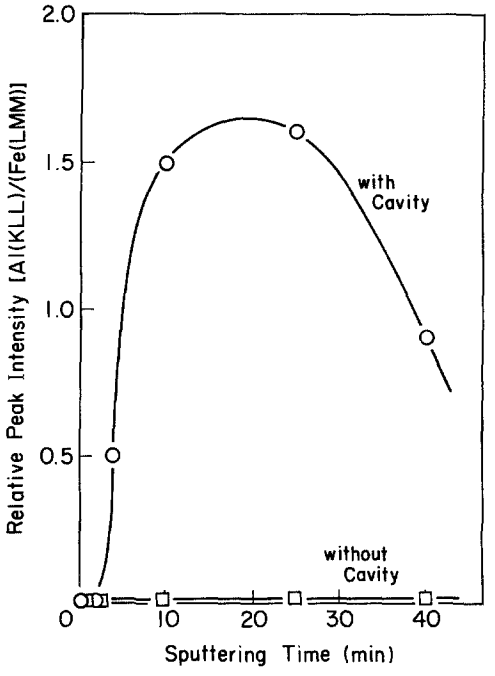

Figure 4 SAM depth profile of aluminium at the interface of oxidized Al-steel.

to study the effects of chromium and/or aluminium enrichment on oxidation.

Fig. 5a shows the depth profiles for chromium, silicon, aluminium and manganese in oxidized Al-steel as a function of the oxygen ion sputter-etching time determined by IMA. Manganese was dissolved in Fe_3O_4, while aluminium, chromium and silicon were enriched in the inner oxide layer. This tendency was most pronounced for aluminium. The depth profiles for oxidized Cr-steel are shown in Fig. 5b for comparison. Manganese was dissolved in the outer Fe_3O_4 layer similar to the Al-steel case. However, the inner oxide layer was not enriched with aluminium or silicon, but it was enriched with chromium. Comparing the two depth profiles (Figs. 5a and b) it can be seen that the inner oxide layer in the Al-steel, which is enriched with impurities, is thicker than that in the Cr-steel.

The above results obtained with the IMA also indicate that the inner oxide layer enriched with aluminium somehow acts as a cavity source and initiation region for the oxide spallation. The depth profile data for the Cr–Al-steel were excluded here, because it was similar to the profile of the Cr-steel.

The micro-Vickers hardness values for the oxides on Al-steel and Cr-steel were 105 and 87 MHv, respectively. This fact also indicates that the oxide on Al-steel is harder and more brittle.

4. Discussion

4.1. Factors affecting adherence of the oxide

Factors to be considered concerning oxide spallation include the following [15]

1. Stress in mono-oxide.
2. Adherence of the oxide to the base metal.

Stresses produced during oxide generation arise from factors such as the difference between the molar volume of the oxide and metal, differences in crystal orientation, recrystallization of the oxide and the contraction of the oxide by point defects [15, 16]. Oxide adherence at the interface can be affected by factors such as gas bubble production by the oxidation of carbon, vacancy injection into the metal from non-stoichiometric oxides like Fe_3O_4 and out-diffusion of iron atoms [1, 2, 17–19].

Since the molar volume of the oxides, usually indicated by the Pilling–Bedworth ratio [16], is the same for both the Al-steel and the Cr-steel, the stress created by the difference between the oxide molar volume and metal is not considered to be the primary reason for the present oxide spallation phenomenon. There is no difference between the crystal orientation of the oxide on the Al-steel and that on Cr-steel, so it is not the primary reason either. Furthermore, it is believed that any recrystallization stress in the oxide is similar on each steel and that contraction of the oxides is less than 0.1% [15]. Thus, factors relating to stresses generated during mono-oxide formation cannot explain the spallation phenomenon.

Cavities, generated at the oxide–metal interface have often been considered to be caused by the oxidation of carbon, the vacancy injection and the out-diffusion of iron atoms. With the ultra low carbon steels, void generation by oxidation of carbon is impossible [19]. Since Fe_3O_4, which comprises most of the oxide, is a p-type semiconductor with a cation-deficient structure it contains cation vacancies. With thick oxide films, Boggs and Kachik [1] and other authors reported that vacancies were injected into the Fe_3O_4–Fe interface to produce cavities. However, this phenomenon might not occur because the present oxides were very thin.

Relative to the adherence of oxide to the metal, it was previously observed on the Al-steel samples that the Fe_3O_4 consisted of double layers, and that spallation occurred at the outer–inner oxide layer interface. Also, it was observed that many cavities existed at this interface and that aluminium was enriched in the inner thick oxide layer. Considering these results, the hypothesis that CO_2 or O_2 gas, with access to the oxide–metal interface through cracking and/or grain boundaries in the oxide, may internally oxidize the metal and create an inner oxide layer [20], is applicable to the present work. Enriched impurities (chromium, aluminium or silicon) may be the key components in the initially generated oxide (the thickness may be less than 1 μm), whichever involves pores or boundaries.

TABLE II The ratio of the ion peak intensities of enriched elements to the $^{57}Fe^+$ peak at the annealed steel surfaces with IMA. (Sputter-etched by an oxygen ion beam, $^{57}Fe^+$ peak = 1000)

	$^{52}Cr^+$	$^{27}Al^+$	$^{28}Si^+$	$^{55}Mn^+$	$^{24}Mg^+$	$^{22}Na^+$	$^{39}K^+$	$^{40}Ca^+$	$^{31}P^+$
Cr-steel	92	0.2	1.1	120	3.2	7.0	5.4	7.0	≈ 0
Al-steel	0.9	42	0.7	95	1.3	6.6	4.2	9.4	≈ 0

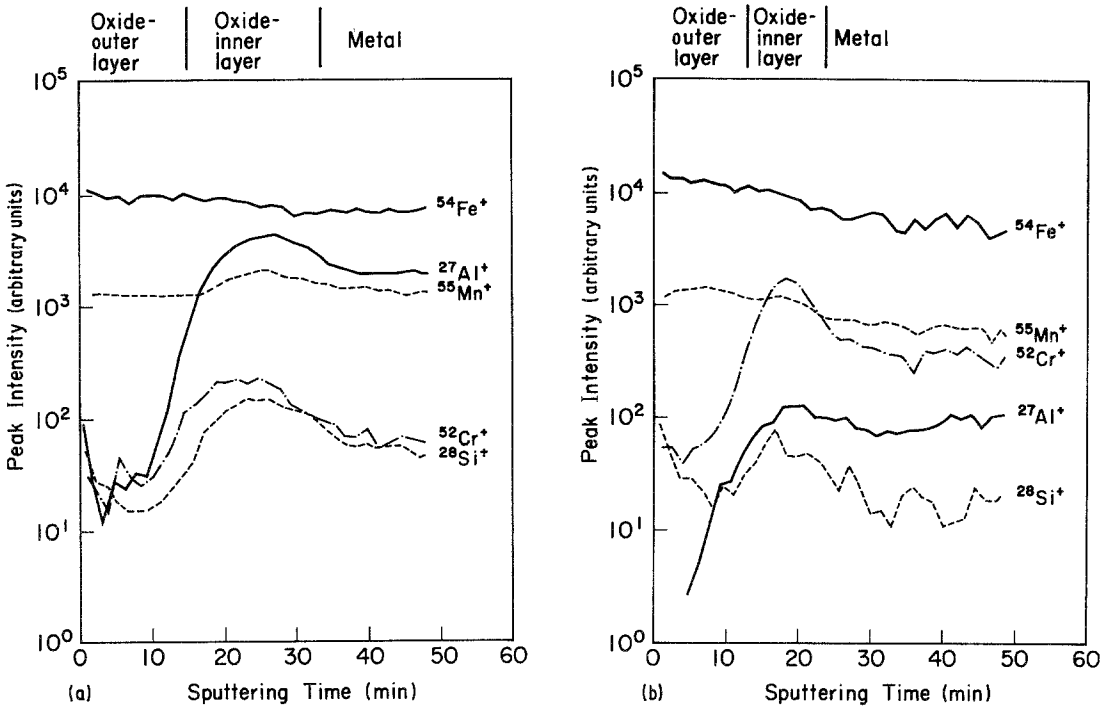

Figure 5 IMA depth profiles of chromium, silicon, aluminium and manganese in oxidized steels. (a) Al-steel, (b) Cr-steel.

This factor is discussed in more detail in the next sections.

4.2. Model for oxidation

As no previous oxidation investigations in the mixed gas (CO_2 + N_2) have been reported, it is difficult to compare the present work with the investigation published by other authors. However, the authors believe that the oxidation of Al-steel can be explained by an internal oxidation by CO_2 and/or O_2.

By virtue of cracking and/or grain boundaries in these coarse and fragile oxides, CO_2 (or O_2) gas has access to the oxide–metal interface. According to work by Gibbs [21], an inner oxide layer at the oxide–metal interface is produced by the reaction $3Fe + 4CO_2 \rightarrow Fe_3O_4 + 4CO$ or $3Fe + 2O_2 \rightarrow Fe_3O_4$. We believed that aluminium enrichment influences the generation of the initial (very thin and rough) oxide which contains many cracks, pores and boundaries, when the Al-steel was first oxidized in 10% CO_2–90% N_2 gas, and that internal oxidation subsequently occurred in 10% CO_2–10% O_2–80% N_2 gas by the transport of CO_2 or O_2 gas through this initial oxide. Newly generated inner oxide may produce a stress at the outer–inner oxide layer interface and the resultant formation of cavities. The thermal cycle of heating and cooling may also include a stress due to the differences in coefficients of thermal expansion. With cavity formation causing the oxide to become less adherent, the outer oxide layer is easily spalled under the influences of these two stresses. If aluminium was not enriched at the interface, the tendency of the initial oxide toward fragility and coarseness and the generation of inner oxide or cavities could be prevented.

In the case of the Cr-steel (diffusion coefficient of chromium in steel is greater than that of aluminium) chromium may also serve as a barrier for aluminium enrichment, as the inner oxide layer on Cr–Al-steel was thin and oxide spalling was not very obvious (Fig. 2). The oxide on Cr-steel grew perpendicularly to the metal surface to form a single Fe_3O_4 layer. Therefore, it can resist the thermal-cycle stress and the spallation. The effect of chromium enrichment may be the generation of an initial outer oxide involving few cavities, pores and boundaries.

5. Conclusions

The authors investigated the effects of trace impurities on the adherence of oxide to ultra low carbon steel. The results are summarized as follows.

1. The spallation of oxide on Al-steel occurred at the outer–inner oxide interface, where many cavities appeared and aluminium was enriched.
2. Aluminium in Al-steel was enriched in the inner oxide layer, while chromium in Cr-steel was enriched in the inner layer and restricted the enrichment of aluminium. However, the inner layer on Al-steel was thicker than that on Cr-steel, because the transport of CO_2 or O_2 gas through the fragile and rough outer layer resulted in internal oxidation of the substrate metal. The generation of the outer layer and the transport of gases were influenced by the aluminium enrichment at the surface on H_2 annealing.
3. The addition of chromium to Al-steel improved the adherence of the oxide to the metal.

Acknowledgements

The authors would like to thank Dr K. Suzuki for his advice and assistance during the final reading of the manuscript, and express their sincere gratitude to Mrs M. Kihara, H. Ohara, K. Saito and O. Hirao who provided or analysed samples.

References

1. W. E. BOGGS and R. H. KACHIK, *J. Electrochem. Soc.* **116** (1969) 424.

2. J. E. ANTILL, K. A. PEAKALL and J. B. WARBURTON, *Corros. Sci.* **8** (1968) 689.
3. G. J. BILLIGNS, M.S. Thesis, "Oxidation and Decarburization Kinetics of Iron–Carbon Alloys in Carbon Dioxide–Carbon Mono-oxide Atmospheres" (McMaster University, Hamilton, Ontario, 1966).
4. K. HAUFFE, "Oxidation of Metals" (Plenum Press, New York, 1965) p. 102.
5. R. J. HUSSEY and M. J. GRAHAM, *Corros. Sci.* **21** (1981) 255.
6. P. BERGE, C. RIBON and P. SAINT PAUL, *Corrosion* **33** (1977) 173.
7. L. TOMLINSON, *ibid.* **37** (1981) 591.
8. D. CAPLAN, R. J. HUSSEY, G. I. SPROULE and M. J. GRAHAM, *Corros. Sci.* **21** (1981) 689.
9. D. CAPLAN and M. COHEN, *ibid.* **7** (1967) 725.
10. V. LEROY, *Mater. Sci. Eng.* **42** (1980) 289.
11. A. RAHMEL and J. TOBOLSKI, *Corros. Sci.* **5** (1965) 333.
12. C. W. TUCK, M. ODGERS and K. SACHS, *Corros. Sci.* **9** (1969) 271.
13. H. NAKAGAWA, Y. UJIHIRA and M. INABA, *Nucl. Instr. Meth.* **196** (1982) 573.
14. B. TAMAMUSHI, "Rikagaku Jiten", 3rd Edn. (Iwanami Shoten Co., Tokyo, Japan, 1971) p. 515.
15. T. HONMA, *Boshyoku Gijutsu* **25** (1976) 251.
16. S. OHARA, "Kinzoku Soshikigaku Gairon" (Asakura Shoten Co., Tokyo, Japan, 1966) p. 144.
17. O. KUBASCHEWSKI and B. E. HOPKINS, "Oxidation of Metals and Alloys", 2nd Edn. (Butterworths, London, 1965) p. 54.
18. J. E. HARRIS, *Acta Metall.* **26** (1978) 1033.
19. R. H. BRICKNELL and D. A. WOODFORD, *ibid.* **30** (1982) 257.
20. A. BRUCKMAN, *Corros. Sci.* **7** (1967) 51.
21. G. B. GIBBS, *Oxidations Met.* **7** (1973) 173.

Received 15 February
and accepted 21 May 1985